Available online at www.sciencedirect.com
SCIENCE DIRECT®
International Journal of Solids and Structures 42 (2005) 681–695
INTERNATIONAL JOURNAL OF SOLIDS and STRUCTURES
www.elsevier.com/locate/ijsolstr

Fracture initiation associated with chemical degradation: observation and modeling

Byoung-Ho Choi [a], Zhenwen Zhou [a], Alexander Chudnovsky [a,*], Salvatore S. Stivala [b], Kalyan Sehanobish [c], Clive P. Bosnyak [c]

[a] *Fracture Mechanics and Materials Durability Laboratory, Department of Civil and Materials Engineering (M/C 246), University of Illinois at Chicago, 2095 ERF, 842 West Taylor Street, Chicago, IL 60607-7023, USA*
[b] *Department of Chemistry and Chemical Biology, Stevens Institute of Technology, Hoboken, NJ 07030, USA*
[c] *The Dow Chemical Company, Freeport, TX 77541, USA*

Received 20 April 2004; received in revised form 14 June 2004
Available online 3 September 2004

Abstract

The fracture initiation in engineering thermoplastics resulting from chemical degradation is usually observed in the form of a microcrack network within a surface layer of degraded polymer exposed to a combined action of mechanical stresses and chemically aggressive environment. Degradation of polymers is usually manifested in a reduction of molecular weight, increase of crystallinity in semi crystalline polymers, increase of material density, a subtle increase in yield strength, and a dramatic reduction in toughness. An increase in material density, i.e., shrinkage of the degraded layer is constrained by adjacent unchanged material results in a buildup of tensile stress within the degraded layer and compressive stress in the adjacent unchanged material due to increasing incompatibility between the two. These stresses are an addition to preexisting manufacturing and service stresses. At a certain level of degradation, a combination of toughness reduction and increase of tensile stress result in fracture initiation. A quantitative model of the described above processes is presented in these work. For specificity, the internally pressurized plastic pipes that transport a fluid containing a chemically aggressive (oxidizing) agent is used as the model of fracture initiation. Experimental observations of material density and toughness dependence on degradation reported elsewhere are employed in the model. An equation for determination of a critical level of degradation corresponding to the offset of fracture is constructed. The critical level of degradation for fracture initiation depends on the rates of toughness deterioration and build-up of the degradation related stresses as well as on the manufacturing and service stresses. A method for evaluation of the time interval prior to fracture initiation is also formulated.

Keywords: Microcrack network; Chemical degradation; Fracture initiation; Material density change; Fracture toughness

* Corresponding author. Tel.: +1 312 996 8258; fax: +1 312 996 3428/+1 312 996 2426.
E-mail address: achudnov@uic.edu (A. Chudnovsky).

0020-7683/$ - see front matter © 2004 Elsevier Ltd. All rights reserved.
doi:10.1016/j.ijsolstr.2004.06.028

1. Introduction

Relatively fast crack propagation in metals exposed to a combined action of constant load (creep condition) and corrosive environment was observed long ago and named "stress corrosion cracking" (SCC). It was recognized later that SCC is a common problem for metals, polymers and composites that serve under a combination of mechanical stress and chemically aggressive (for material in question) environment (Volman et al., 1996). There is a specific molecular level pathway of SCC for each material-environment system. At the same time, there is also a striking commonality of the phenomena in different material-environment systems, when it is considered on a continuum mechanics/thermodynamics level. In this paper, we develop a model of SCC, considering chemical degradation by oxidation, i.e., corrosion of polymers. We address a practical problem of SCC initiation in an internally pressurized plastic pipe that transports fluid, containing a chemically aggressive (oxidizing) agent for a given polymer agent. A similar approach has been applied to modeling SCC in gas pipe grade steels (Zhang et al., 1998, 2000; Choi and Chudnovsky, 2002).

In Section 4 we give a brief exposition of the mechanisms of polymer degradation, and the changes in material properties resulting from the oxidative degradation, as a precursor to SCC. More detailed studies of various mechanisms of polymer degradation stabilization against degradation can be found for example in a number of publications (Allara and Hawkins, 1978; Allen, 1983; Guven, 1990; Ivanova et al., 1995; Bishop et al., 2000). The objective of this study is a quantitative modeling of the effect of chemical degradation of polymers on mechanical properties, such as strength, toughness, rigidity as well as on fracture initiation and growth.

2. Observation of SCC in plastic pipes

SCC initially appears in the form of a microcrack network that evolves into a colony of cracks. There are numerous patterns of SCC colony that usually reflects the principle stress and/or maximum shear stress trajectories in the domain exposed to aggressive environment. A few examples of SCC patterns are shown in Figs. 1–4. Fig. 1a depicts a microcrack network on the inner surface of a thermoplastic pipe. The microcracks have formed an irregular cell pattern oriented along maximum shear stress directions. The main crack visible on the micrograph follows the axial direction of the pipe, i.e., minimal principle stress direction in the internally pressurized pipe (Fig. 1a). Apparently, it is formed by coalescence of microcracks and has a clear zigzag shape well visible in Fig. 1b, the magnified domain "L" in the center of Fig. 1a. A random microcrack network with an irregular rectangular cell pattern resulting primarily from degradation-induced stresses is depicted in Fig. 2. Here the microcrack orientation coincides with that of the principle stresses. Some microcracks have started to merge, forming small clusters, a precursor of the macroscopic crack. A macroscopic crack along the axial direction of the pipe is shown in Fig. 3. The dominant service hoop stress is responsible for the orientation of this crack. A number of circumferential hairline cracks perpendicular to the main crack apparently have been formed before the main crack opening. It follows from continuous lines of the cracks on both side of the main crack (Fig. 3). These cracks are formed within a relatively thin layer of highly degraded material that partially flakes off the surface. The shapes of SC crack according to the section view are shown in Fig. 4.

The patterns shown above illustrate that the mechanical stresses control the fracture orientation, though the chemical degradation plays the leading role in the fracture process). It is commonly accepted for various engineering materials, including plastics, that SCC results from strongly coupled electro-chemical and thermo-mechanical processes, and sensitive to material composition, morphology and residual stresses (e.g., Volman et al., 1996). Generally, one can distinguish four stages of SCC: (1) microcracks initiation; (2) slow growth of individual cracks; (3) strong interaction of cracks and clusters formation; and (4) clusters growth

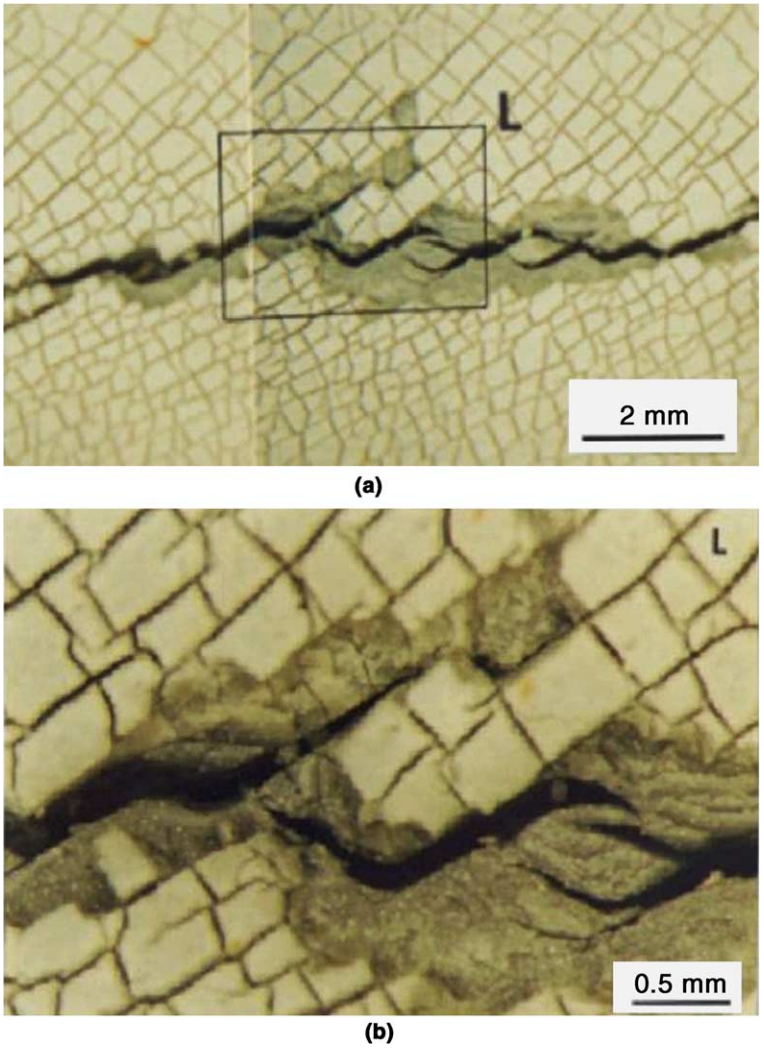

Fig. 1. Microcrack network on the inner surface with irregular cell pattern. (a) General view of microcrack network. (b) Higher magnification of domain L from (a).

and instability (Choi et al., 2002). In what follows, we address only the first stage, i.e., the fracture initiation process.

3. Fracture initiation conditions

In the examples of SCC shown previously, the orientation of fracture and kinetics of fracture growth obey deterministic laws, whereas the time and location of individual microcrack initiation site are essentially random events. There are random variations of chemical composition and material morphology from one point to another, which leads to a random spatial fluctuation of the degree of material degradation. Let ω ($0 \leqslant \omega \leqslant 1$) represent a degradation parameter at a given point $\underline{x}$ at the instance of time, t. Apparently, ω

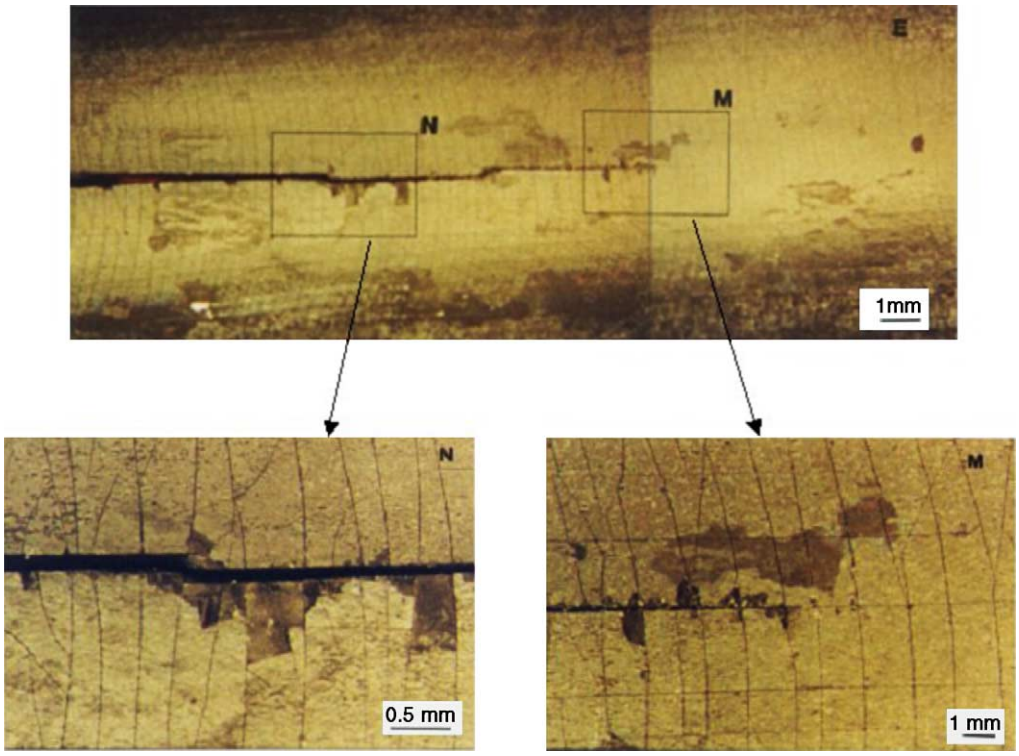

Fig. 2. Main through crack along the axial direction of pipe and shallow circumferential cracks.

(x,t) is a random field. The spatial variation of ω is analogous to the thermal fluctuations in time considered in classical theory of nucleation (Anismov, 2003). However, fracture initiation, is an essentially irreversible event, and in this sense, is different from thermodynamic nucleation of a new phase. Here, we consider an alternative to classical nucleation theory approach in modeling of fracture initiation by means of Statistical Fracture Mechanics (Chudnovsky, 1973; Chudnovsky and Kunin, 1987). We define fracture initiation (FI) as *an event of spontaneous expansion to a macroscopic scale of a brittle fracture (a crack) triggered by a random defect formed on a sub-microscopic scale*.

As an example, in this paper we consider FI due to chemical degradation of polybutylene (PB) tubing, employed in potable water distribution systems. Certain disinfectants added to the water create an aggressive for PB environment, which with time results in formation of a layer of degraded material of thickness l_0 adjacent to the inner surface. The degradation process affects the fracture initiation in two ways: it causes a significant decay of specific fracture energy $\gamma(\omega)$ and a buildup of degradation related stress σ_ω as a noticeable part of total stress σ_{tot}. The fastest rate of degradation in this case takes place at the inner surface of the tubing, which is in direct contact with the flowing water. Therefore the first, sub-microscopic defect that triggers FI is, most likely, located at the inner surface. FI in this case means a *spontaneous expansion of brittle fracture (a crack) from a random sub-microscopic defect at the inner surface across the degraded layer of l_o thickness*. A small domain of a circumferential cross section of PB tubing is shown on the micrograph in Fig. 5a. The micrograph displays a layer of degraded polymer (lighter color) adjacent to the inner surface of the tubing. A boundary that separates the degraded and undegraded (original) materials is also well visible due to the differences in color. One can see multiple fractures initiated at the inner surface of the tubing and extended through the degraded layer (Fig. 5a). Fig. 5b is a schematic representation of a sample set Ω

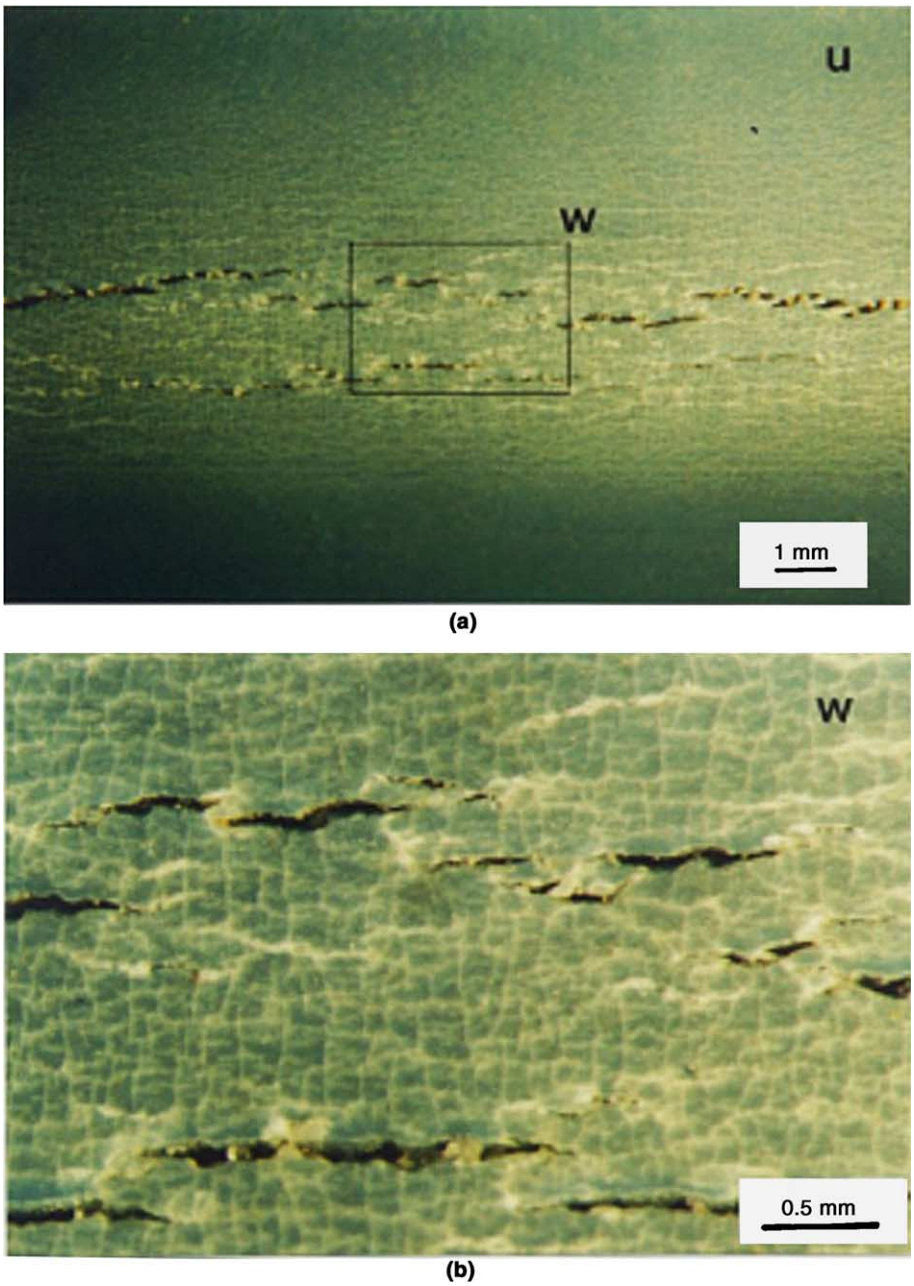

Fig. 3. Microcrack network with an irregular rectangular cell pattern and randomly distributed axial cracks. (a) Microcrack network with macro axial crack. (b) Higher magnification of domain W from Fig. 1(a).

of random fracture paths, that may be constructed considering a large number of cracks shown in Fig. 5a shifted toward one origin, $\underline{x}_0$. Apparently, only one particular path $w(\underline{x})$ from the set Ω of virtual paths is realized in each particular location. Moreover, the stress release resulting from fracture formation determines almost regular spacing between individual fractures visible in Fig. 5a.

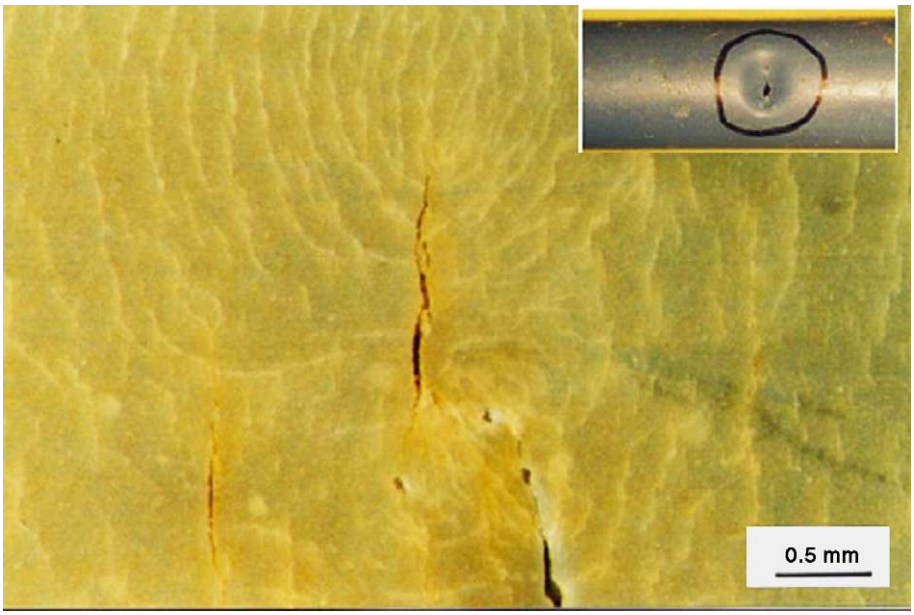

Fig. 4. Microcrack network on the inner surface of the pipe caused by a combination of polymer degradation and a stress field in a vicinity of crack.

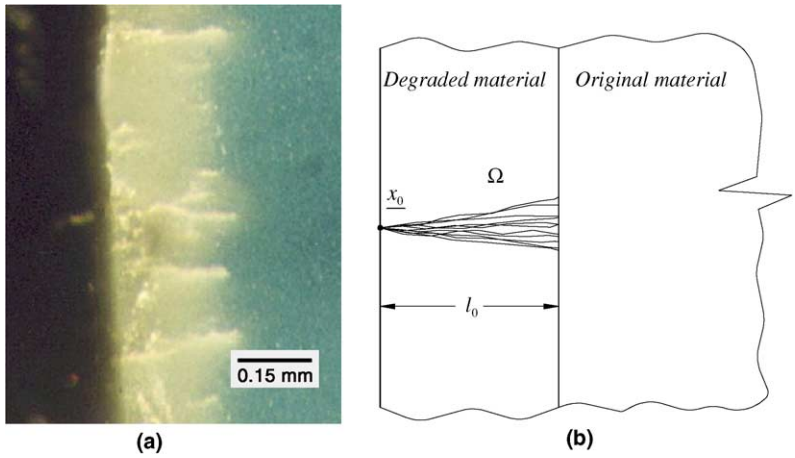

Fig. 5. Optical photo and schematic of random trajectories of crack initiation. (a) Optical photo of crack initiation. (b) Random trajectories of crack initiation.

Let consider a fracture path $w(\underline{x})$ that starts at a point $\underline{x}_0$ on the inner surface and terminates at a point $\underline{X}$ on the interface between degraded and undegraded material (see Fig. 5b). The condition of fracture extension form $\underline{x}_0$ to $\underline{X}$ along $w(\underline{x})$ is the requirement that Griffith condition ($G_1(x) \geqslant 2\gamma(\underline{x})$) *is met at every point of fracture trajectory* $w(\underline{x})$. Here G_1 is the conventional energy release rate (ERR) that depends on total stress and the geometry of fracture path $w(\underline{x})$. The specific fracture energy $\gamma(\underline{x}, \omega(\underline{x}, t))$ is apparently a random field that reflects a random variation on the microscopic and sub-microscopic scales of the chemical

composition and morphology of the material as well as the extent of degradation, ω. The above condition of FI, i.e., fracture extension from $\underline{x}_0$ to $\underline{X}$ along $w(\underline{x})$ is the only meaningful generalization of Griffith condition for a heterogeneous random media with a random field of specific fracture energy $\gamma(\underline{x})$.

Consider fracture triggered at a point $\underline{x}_0$, where either a preexisting defect or one formed by most intense degradation is located (see Fig. 5). According to experimental observations, this point is most likely located at the inner surface of the tubing. From that point of origin, the fracture expands in a brittle manner (as a crack) across the layer of material degradation. The thickness l_0 of degraded layer is relatively small (usually between 50 and 150 μm) in comparison to the inner diameter of the tubing (between 10 and 22 mm). Thus, a depth of the fracture is much smaller than its width (about two orders of magnitude), which means a plain strain (2D) problem can be considered. Consider a set Ω of random mutually exclusive fracture trajectories $\{w(\underline{x})\}$ that start at the fracture origin $\underline{x}_0$ and extend to the point $\underline{X}$ at the interface between the degraded layer and the original material (see Fig. 5). The probability of fracture initiation $P\{\mathrm{FI}\}$, i.e., the probability of spontaneous fracture extension from $\underline{x}_0$ to $\underline{X}$, is given by the sum over Ω of conditional probability $P_w(\underline{x}_0, X/w)$ of fracture formation along the particular path $w(\underline{x})$ multiplied by the probability $P\{\omega\}$ of the particular path $w(\underline{x})$ to be selected by chance from the set of all possible paths Ω (Chudnovsky, 1973; Chudnovsky and Kunin, 1987):

$$P\{\mathrm{FI}\} = \sum_{\Omega} P_{\mathrm{w}}(\underline{x}_0, \underline{X}/w) \cdot P\{w\}. \tag{1}$$

Since Ω is an innumerable set, the summation in (1) is a symbolic expression. It implies a functional integration over Ω with respect to an appropriate measure that accounts for the roughness (Hausdorf dimension) of fracture trajectories (Chudnovsky, 1973; Chudnovsky and Kunin, 1987).

The conditional probability $P_w(\underline{x}, \underline{X}/w)$ of fracture extension from $\underline{x}$ through $\underline{X}$ along a particular path $w(\underline{x})$ is defined as the probability that Griffith condition ($G_1 \geqslant 2\gamma$) for an infinitesimal crack extension is met *at every point* along the path $w(\underline{x})$ between $\underline{x}$ and $\underline{X}$. A straight forward probabilistic considerations presented in Chudnovsky (1973) and Chudnovsky and Kunin (1987) lead to the following expression for $P_w(\underline{x}, \underline{X}/w)$:

$$P_{\mathrm{w}}(\underline{x}, \underline{X}/w) = \exp\left\{ -\int_{\underline{x}}^{\underline{X}} \mathrm{Prob}\{2\gamma(\xi) \geqslant G_1(\xi)\} \frac{\mathrm{d}\xi}{r} \right\}, \tag{2}$$

where r stands for the correlation distance of γ-field and the integration in (2) is performed along the fracture path $w(\underline{x})$:$\mathrm{d}\xi = w'(\underline{x})\,\mathrm{d}x$. Since the fracture path $w(\underline{x})$ is formed by a crack "selecting" the weakest direction at each step of its advance, the pointwise distribution of γ-field *along the fracture path* $w(\underline{x})$ follows a minimal values distribution. The Weibull distribution is a natural choice of such a distribution:

$$F_\gamma = \begin{cases} 0 & \text{if } \gamma \leqslant \gamma_{\min}, \\ 1 - \exp\left[-\left(\frac{\gamma - \gamma_{\min}}{\gamma_0} \right)^{\alpha} \right], & \text{for } \gamma > \gamma_{\min}, \end{cases} \tag{3}$$

where $\gamma_{\min}$, γ_0 and α are well known shift, scale and shape parameters of Weibull distribution. A decrease of the specific fracture energy $\gamma(\omega)$ with degradation is reflected in $\gamma_{\min}$, γ_0 and α dependence on the degradation parameter ω. The scale factor γ_0 is simply related to the mathematical expectation $\langle\gamma\rangle$ of γ-field: $\gamma_0 = \Gamma^{-1}(1+\alpha)\langle\gamma\rangle(1-q)$, where Γ stands for Γ-function of $1 + \alpha$, and q is the ratio of $\gamma_{\min}/\langle\gamma\rangle$.

Substituting (2) and (3) in (1) and performing the "summation", i.e., a functional integration in (1) with an appropriate measure that reflect the roughness of observed fracture trajectories, one determines the probability of fracture initiation $P\{\mathrm{FI}\}$. A method to compute $P\{\mathrm{FI}\}$, i.e., the probability of spontaneous crack propagation from $\underline{x}_0 = 0$ to $\underline{X} = l_0$ under the total tensile stresses σ_{tot} have been presented (Chudnovsky, 1973; Chudnovsky and Kunin, 1987). The Monte Carlo method can be applied for fracture trajectories with an arbitrary roughness (Chudnovsky et al., 1997). When fracture paths follow the Brownian particle

trajectories, an evaluation of the functional integral is reduced to solution of diffusion type partial differential equations, (so called "diffusion approximation"). In the first approximation, when the roughness of fracture path is ignored, $P\{\mathrm{FI}\}$ is simply expressed as:

$$P\{\mathrm{FI}\} = \exp\left[-\int_0^{l_0} \exp\left\{-\left[\frac{G_1(\underline{x},\sigma_{\mathrm{tot}}) - 2\gamma_{\min}}{2\gamma_0}\right]^{\alpha}\right\}\frac{\mathrm{d}x}{r}\right], \tag{4}$$

ERR G_1 for the problem at hand (Fig. 5b) can be expressed as $G_1 = (1.12\sigma_{\mathrm{tot}})^2\pi x E'^{-1}$, where $E' = E(\omega)/(1-\nu^2(\omega))$, E and ν stand for the Young's modulus and Poisson's ratio, both weakly dependent on degradation parameter ω, and the total stress σ_{tot} comprises of residual (manufacturing related) stresses, service stresses σ_0, and degradation induced stresses σ_ω. Thus, $P\{\mathrm{FI}\}$ (4) depends on ω in many ways and can be written as $P\{\mathrm{FI},\omega\}$. We define a critical level of degradation ω^* as the value of the degradation parameter ω, at which fracture initiation takes place with certainty, $P\{\mathrm{FI}\} = 1$. Then cumulative distribution $F(\omega^*)$, as well as the statistical moments of ω^* (mathematical expectation $\langle\omega^*\rangle$, standard deviation $\sigma(\omega^*)$, etc.) can be computed using (4):

$$F(\omega^*) = P\{\mathrm{FI},\omega\}|_{P\{\mathrm{FI}\}=1}, \quad \langle\omega^*\rangle = \int_0^1 \omega^* \mathrm{d}F(\omega^*), \quad \sigma^2(\omega^*) = \int_0^1 (\omega^* - \langle\omega^*\rangle)^2 \mathrm{d}F(\omega^*). \tag{5}$$

The original material has sufficient toughness $2\gamma_0$ to make the crack nucleation practically an impossible event. However, there is a decrease of $\gamma(\omega)$ and an increase of σ_{tot} with progression of degradation (increasing ω). Thus, the probability of crack nucleation increases to the certainty ($P\{\mathrm{FI}\} = 1$) with ω approaching the critical value of ω^*. The kinetics of the process of degradation in time $\omega(t)$ together with the value of ω^* allows one to determine the time t_i of fracture initiation considered below in Section 7.

4. Chemical degradation of engineering thermoplastics

Polymers consist of long-chain molecules (macromolecules) formed by the chemical union (polymerization) of single units (monomers). The monomers can be of single or multiple types. The properties of polymers are governed to a large extent by the chemical makeup, molecular architecture and supramolecular architecture (such as crystal morphology). Engineering thermoplastics are plastics which can be reheated and reshaped for load-bearing applications, often for use over a significant lifetime. As the polymerization proceeds, the size of the growing chain increases. It is commonly characterized by molecular weight, MW (g/mole), which represents the weight (in grams) of Avogadro's number (6×10^{23}) of molecules. As a consequence of the polymerization there is often a distribution of chain lengths. This distribution is characterized by the moments of molecular weight distribution: the first moment, or number average $\mathrm{MW_n}$, ($\overline{M}_{\mathrm{n}} = N_iM_i/N_i$, where N_i is the number of chains with molecular weight M_i); the second moment the weight-average MW ($\overline{M}_{\mathrm{w}} = \sum N_iM_i^2/\sum N_iM_i$) and so on.

The aggregate state of polymers and practical applications are directly related to the size of the molecules, as it is illustrated below using as an example the hydrocarbon molecules of chemical structure H–$(CH_2)_n$–H, where H and C stand for hydrogen and carbon respectively, and n is the number of repeated units –CH_2–. Table 1 show the effect of the number n of monomers in the chain on the physical state and useful applications of the poly(hydrocarbon)s.

The useful properties of polymers depend not only on an average MW, but also on the MWD. The ratio $\overline{M}_{\mathrm{w}}/\overline{M}_{\mathrm{n}}$ is usually taken as a measure of the width of the distribution or the dispersity. For a polydisperse system $\overline{M}_{\mathrm{w}}/\overline{M}_{\mathrm{n}} \geqslant 1$. The reduction of MW during degradation is usually followed by a reduction of dispersity as well. It should be mentioned that both an average MW and MWD may have an effect on the rate of polymers degradation. For example, in the thermal oxidation of the polyethylene samples of identical average MW, but of different MWD, the one with a wider MWD oxidized more readily.

Table 1
Polymer status according to number of monomers

Number n of monomers	Physical state	Application
1–4	Gas	Cooking (methane, $n = 1$); (propane, $n = 3$); generally lighter (butane, $n = 4$)
5–11	Low viscosity liquid	Gasoline, e.g., octane, $n = 8$
11–16	Medium viscosity liquid	Kerosene
16–25	High viscosity liquid	Oil, grease
25–100	Solid	Paraffin wax, candles
>1000	Engineering plastics	Polyethylene bottles, containers, vessels, pipes

A given property, such as tensile and impact strength, toughness, yield strength, melting temperature etc., improve with increasing MW (all other conditions considered to be the same). Conversely, a reduction of molecular weight, i.e., a process of chemical degradation, results in a decay of useful properties. Table 1, when considered from bottom up, is a clear illustration of degradation process (decrease of the number n of monomers in macromolecule and resulting change in the physical state of polymeric material).

Chemical degradation of polymers in a broader sense may be considered as any type of modification of a polymer chain involving the main-chain backbone or side groups, or both. These modifications often result in of breakage of primary valence bonds (chain scission) leading to lowering of molecular weight. As in polymerization, degradation process may proceed via radical or ionic mechanisms, or both. In either case, MW reduction results from random chain scission (random degradation), or by depolymerization that release monomer units in succession progressing from an end of the chain. For example, the hydrocarbon polyolefins (polyethylene, PE; polypropylene, PP; Polybutylene, PB) degrade by random thermal oxidation via a free radical mechanism, whereas poly(tetrafluoroethylene) (Teflon; $-(CF_4)_n-$) depolymerizes. Poly(oxymethylene), a tough engineering polymer (Acetal), (POM; $-(OCH_2)_n-$) degrades randomly via free radical mechanism above 270 °C, whereas below 270 °C, it degrades ionically by unzipping and releasing monomer, HCHO (formaldehyde). Polymers that have carbon-carbon double bonds (unsaturated polymers), i.e., paired electrons between carbon atoms, are more susceptible to oxidative degradation than the saturated polymers (one pair of electrons between carbon bands). Additives are generally employed in polymers to provide a certain protection against degradation. Thus, consideration of depletion of these additives is a critical factor to be considered when understanding lifetime of polymers in various applications.

The specific example of degradation related fracture initiation considered in this paper deals with polyolefin pipes (PE, PP, PB) employed in portable water distribution. Disinfectants, such as chlorine (Cl_2) are commonly added to potable water. The chlorine in water undergoes hydrolysis and forms hypoclorous acid (HOCl), a strong oxidizing agent. In water, the hypoclorous acid, in its turn, dissociates producing the hypochlorite ion (OCl^-): $HOCl \leftrightarrow H^+ + OCl^-$.

The double arrow above indicates that the reaction proceeds in both directions. When the equilibrium is attained, both HOCl and OCl^- co-exist, with the equilibrium ratio dependent on the pH of the aqueous solution. At about neutral pH (pH $\sim$ 7) the concentrations of HOCl and OCl^- are equal. The equilibrium is shifted toward HOCl at pH below 7 (acidic water), and toward OCl^- at pH above 7, (alkaline water). Since HOCl is a much stronger oxidizing agent than OCl^-, chlorine in acidic water is more aggressive than that in alkaline solution. In addition to HOCl and, portable water contains dissolved molecular oxygen and various types of impurities, such as multi-valent metals and theirs ions, e.g., copper, iron, chromium, which catalyze the decomposition of the hydroperoxides.

Polyolefin pipes, as well as most of other polymer products, are subject to oxidative degradation during their processing and service life. In the processing stage, (e.g., pipe extrusion) the polymer is exposed to very high temperature and to air. In service, the pipes are exposed to chemically aggressive environment discussed above. Therefore, small quantities of stabilizers (between 0.1% to 1.0%) are incorporated in

polyolefin pipes, as well as in all commercial plastics. The main function of stabilizers (antioxidants) is to postpone the onset of degradation and to slow down the rate of degradation. The efficiency of stabilizers depends on their type, concentration and combination of different stabilizers in the package. In polyolefin pipes employed in portable water distribution, the stabilizers are being depleted with time (consumed and leached out) from the inner surface layer, which is in contact with the flowing water. The loss of stabilizer renders the inner surface susceptible to degradation.

The oxidative degradation of polyolefin pipe does not start immediately after the contact of the polymer with potable water. There is long induction period during which the depletion of stabilizers and a slow rate of oxygen absorption, accompanied by a slight rise in temperature, take place. In addition, carbonyl and hydroperoxides are formed at concentrations that tend toward equilibrium. At the end of the induction period, characterized as the oxidation induction time (OIT), an abrupt transition occurs; when oxygen-uptake increases at an accelerating rate and temperature rises rapidly. OIT represents the time necessary for a significant depletion of stabilizers and built-up of a sufficient quantity of hydroperoxides, which subsequently decompose at an accelerating rate.

Mechanical stresses imposed upon plastics exposed to chemically aggressive environment as well as various types of impurities in the water may reduce OIT and accelerate the rate of oxidative degradation.

A number of experimental techniques have been develop to detect the oxidative degradation by detecting the products of oxidation (e.g., infra-red spectroscopy (IR)) and to quantify extend of degradation by direct (e.g., gel permeation chromatography (GPC)) or indirect (Viscometry) evaluation of MW reduction.

Quantitative modeling of chemical degradation and resulting deterioration of material properties one needs to introduce a degradation parameter, to monitor its evolution, and to establish relationship between the degradation parameter and material properties in question. A simple and easy measurable degradation parameter $\omega(t)$ is naturally to express in terms of current and initial number average molecular weights $M_n(t)$ and $M_n(0)$:

$$\omega(t) = 1 - M_n(t)/M_n(0). \tag{6}$$

Here we use the number average MW as more directly linked to deterioration of strength and toughness, instead of weight average MW employed in the similar parameter recently introduced in Niu et al. (2000). Reduction of molecular weight, i.e., increase of the degradation parameter ω leads to an increase of crystallinity in semicrystalline polymer as well as density, a subtle increase in yield strength, and a dramatic reduction in toughness. The relationships between degradation parameter and crystallinity, density, and toughness of PB, a semicrystalline engineering thermoplastic from the polyolefin family, have been recently studied using a UV accelerated oxidation technique (Niu et al., 2000). In that study the weight average molecular weight was measured by solution viscometry; density was measured using density gradient column, and the tensile toughness was evaluated from standard tensile test (ASTM D 638). In the absence of independent measurements, in the present work we use the data reported in Niu et al. (2000) for evaluation of the degradation parameter (6) and relations between the degradation parameter on one side and density and toughness on the other. Since the number average and the weight average MWs have similar power type relations with intrinsic viscosity, directly measured in Niu et al. (2000) for evaluation of MW, we assume that the ratios of the current and initial molecular weights are also similar. The graph of degradation parameter in terms of UV exposure time has a characteristic "sigmoidal" shape reflecting a long oxidation induction time (OIT) prior to a noticeable degradation, then relatively fast oxidation process when $\omega(t)$ changes rapidly, and the final saturation stage, when $\omega(t)$ does not show any noticeable variation (Niu et al., 2000).

The changes in crystallinity, density and toughness vary in time following $\omega(t)$. The material properties variation in terms of a parameter of state $\omega(t)$ rather then in time are presented below based on data reported (Niu et al., 2000). Both, the relative density $\delta\rho/\rho_0$ (in %) and normalized toughness parameter γ/γ_0 variations with degradation parameter ω are shown in Fig. 6. Simple power type relations are used to approximate the experimental data

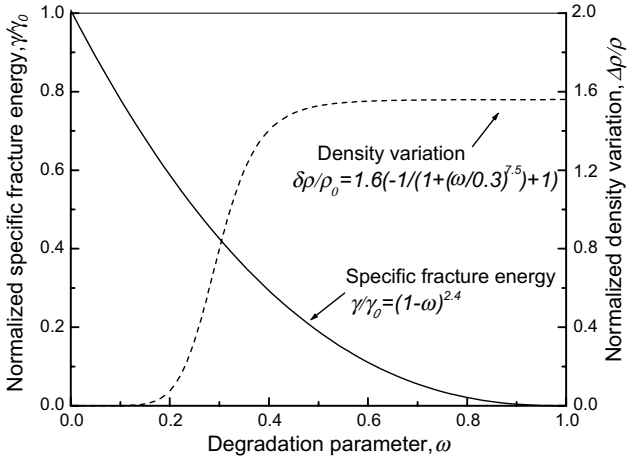

Fig. 6. Normalized toughness, γ/γ_0, and density change, $\Delta\rho/\rho_0$ (in %).

$$\gamma = \gamma_0(1-\omega)^n, \tag{7}$$

$$\delta\rho/\rho_0 = 1.5[11/(1+0.2\omega)^m]. \tag{8}$$

It can be seen from Fig. 6, the most dramatic variation of the material properties occurred before ω reaches 0.5.

5. Degradation related stresses

Increase of density, i.e., shrinkage of the degraded inner surface layer of plastic pipe is constrained by the outer layer of unchanged material. It results in an increase of incompatibility between the inner and outer layers and a buildup of tensile stress within the degraded layer and compressive stress in the outer layer. To evaluate the stresses it is convenient to consider an outward oriented traction $\underline{P}$ along the interface between the inner (degraded) and outer (unchanged) layers that reflects the constraint applied to the inner layer (see Fig. 7). Computation of interfacial traction $\underline{P}$ and degradation related radial $\sigma_{\omega,rr}$; circumferential (hoop)

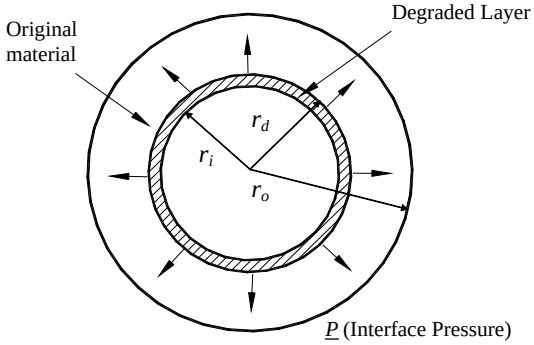

Fig. 7. A sketch of polymer tubing cross section with inner degraded layer.

$\sigma_{\omega,\theta\theta}$ and axial $\sigma_{\omega,zz}$ components of stress tensor follows from the solution of an axisymmetrical, plain strain elasticity problem for traction free thin bimaterial cylindrical shell with a time dependent density of the inner layer, as shown in Fig. 7. The compatibility equation (displacement continuity along the interface between inner and outer layers) together with the conventional equilibrium equations constitutes a complete set of equations for determination of the stress tensor. All stress tensor components, hoop, axial and radial, acting in the degraded layer are proportional to the interfacial traction $\underline{P}$, which explicitly depends on material density variation, pipe dimensions and degraded layer thickness:

$$\underline{P} = \frac{E(\omega)(r_d^2 - r_i^2)(r_0^2 - r_d^2)}{4r_d^2(r_0^2 - r_i^2)} \cdot \frac{\Delta\rho}{\rho}, \tag{9}$$

where r_d, r_i, and r_0 are indicated in Fig. 7. For the problem at hand, the hoop $\sigma_{\omega,\theta\theta}$, radial $\sigma_{\omega,rr}$ and axial $\sigma_{\omega,zz}$ components of stress tensor can be expressed as:

$$\sigma_{\omega,\theta\theta} = \frac{\underline{P} \cdot r_d^2}{r_d^2 - r_i^2}\left\{1 + \left(\frac{r_i}{r}\right)^2\right\}, \tag{10}$$

$$\sigma_{\omega,rr} = \frac{\underline{P} \cdot r_d^2}{r_d^2 - r_i^2}\left\{1 - \left(\frac{r_i}{r}\right)^2\right\}, \tag{11}$$

$$\sigma_{\omega,zz} = \nu(\sigma_{\omega,rr} + \sigma_{\omega,\theta\theta}) = \frac{2\nu \cdot \underline{P} \cdot r_d^2}{r_d^2 - r_i^2}. \tag{12}$$

The circumferential (hoop) stress $\sigma_{\omega,\theta\theta}$ is the dominating stress component induced by degradation. Dependence of the hoop stress $\sigma_{\omega,\theta\theta}$ on the degradation parameter ω is shown in Fig. 8 for three values of degraded layer thickness l_0: 1% (0.02 mm), 3% (0.06 mm) and 5% (0.1 mm) of wall thickness. It can be seen from Fig. 8 that the degraded layer thickness has almost no effect on the magnitude of hoop stress. However, the amount of induced stresses due to chemical degradation is comparable to stresses due to internal pressure, so the possibility of crack initiation will increase faster than predicted considering mechanical loading only.

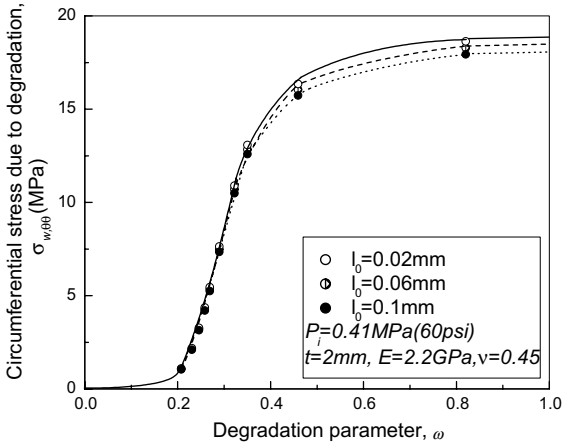

Fig. 8. Maximum hoop stress dependency on degradation level.

6. Evaluation of critical level of degradation ω^*

Cumulative distribution $F(\omega^*)$, as well as mathematical expectation and standard deviation of the critical level of degradation ω^* (5) introduced in Section 3, all depend on the total stresses, particularly stress generated by internal pressure p and degradation related stresses, and the rate of toughness reduction with respect to ω and $\gamma(\omega)$. All these relations are accounted for in Eqs. (4), where σ_{tot} is the sum of (a) hoop stress $\sigma_{0,\theta\theta}(p)$ due to applied internal pressure that does not depend on ω, and (b) degradation induced $\sigma_{\omega,\theta\theta}$ expressed by (9) and (10). The hoop stress $\sigma_{0,\theta\theta}(p)$ in internally pressurized pipe is well known (e.g., Shames and Cozzarelli, 1992):

$$\sigma_{0,\theta\theta} = p\frac{r_i^2}{r_0^2 - r_i^2}\left(1 + \frac{r_0^2}{r_i^2}\right). \tag{13}$$

Employing (10) and (13) for computation of ERR G_1 (we ignore the processing related stresses), and taking $\langle\gamma\rangle$ dependence on ω the same as (7) for various q on degradation parameter ω, into Eq. (4), we find the cumulative distribution $F(\omega^*)$, and the statistical moments of ω^* and their dependence on internal pressure p. The cumulative distribution $F(\omega^*)$ for three values of $q = \gamma_{\min}/\langle\gamma\rangle$ are shown in Fig. 9. The mathematical expectation $\langle\omega^*\rangle$ dependence on internal pressure is depicted in Fig. 10 for various values of q parameter. Apparently, the greater the applied pressure p, the lesser level of degradation is required to initiate fracture.

7. Fracture initiation time

The kinetic equation for the degradation parameter $\omega(t)$ combined with a critical level ω^* of degradation at the onset of fracture leads to determination of time to FI. A simple procedure for evaluation of time to fracture initiation as the result of polymer degradation is presented in Fig. 11. The solid line in Fig. 11 represent the progression of degradation $\omega(t)$ with time. The oxidation induction time t_{OIT} at normal service conditions is taken as the time scale for horizontal axis. There is very little degradation for dimensionless time, $\tau = t/t_{\text{OIT}} < 1$. Beginning from $\tau = 1$ the degradation process rapidly progresses ($\omega(t) \to 1$). The dotted line represents $\langle\omega^*\rangle$ dependence on applied pressure p. The internal pressure p is indicated on the upper horizontal axis. Two values of applied pressure are selected for the illustration of the procedure. The corresponding two levels

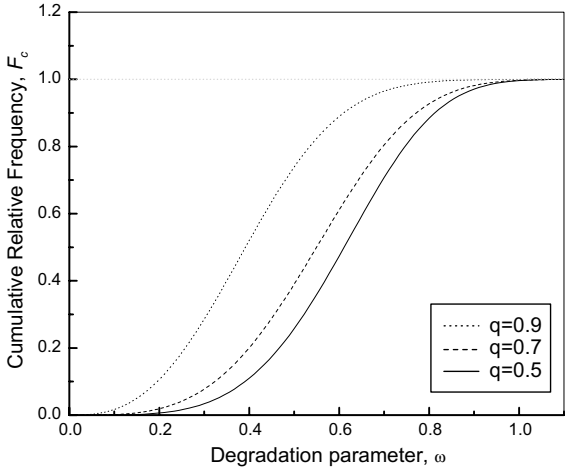

Fig. 9. Cumulative distribution $F(\omega^*)$ for three values of q.

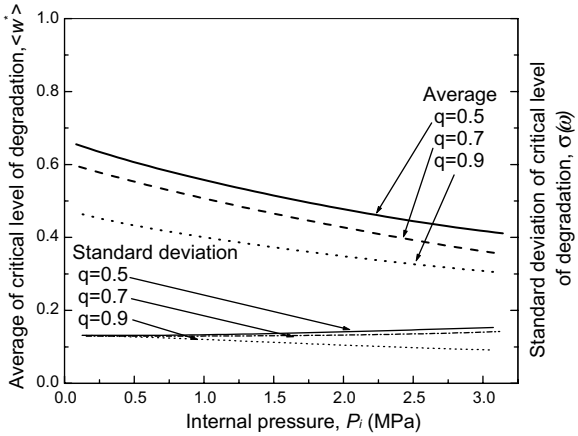

Fig. 10. Critical degradation level ω^* dependence on internal pressure.

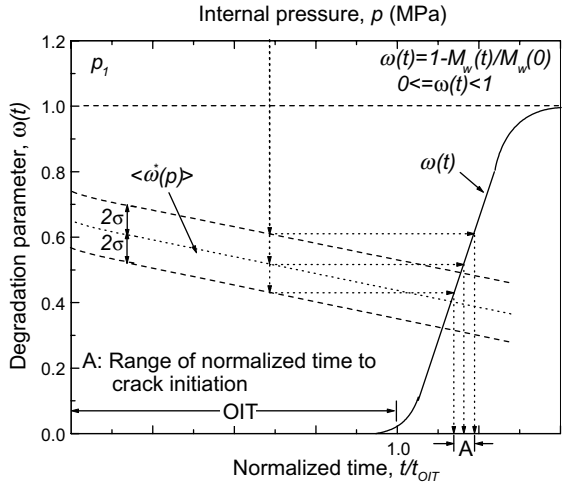

Fig. 11. Schematic diagram for determination of fracture initiation time.

of the average critical degradation parameter $\langle\omega^*\rangle$ are marked on the dotted line of $\langle\omega^*\rangle \sim p$ dependence by vertical arrows. The horizontal arrows indicate $\langle\omega^*\rangle$ levels on the $\omega(t)$ curve. Vertical arrows from these points to the time axis indicate the corresponding time to fracture initiation. The schematic diagram of Fig. 11 for evaluation of the time to fracture initiation suggests that the onset of fracture in PB is primarily controlled by the degradation process and weakly dependent on applied load. At the same time, one should keep in mind that the stresses may affect OIT that is used as a time scale for normalization.

8. Conclusions

The initiation stage of SCC is primarily controlled by the kinetics of chemical degradation. The degradation significantly affects the specific fracture energy and creates a noticeable buildup of degradation re-

lated stresses. The applied pressure may affect the critical level of degradation at the onset of fracture. However, it has a relatively small effect on the time of fracture initiation. The applied load starts to play an increasingly important role with stress corrosion crack growth, crack interaction and formation of clusters (the second and third stages of SCC). Finally, the external load becomes a dominant factor in SCC colony instability and ultimate failure.

There is a challenge to formulate an accelerated test conditions that would be relevant to the observed phenomena. Conventional acceleration by an elevated temperature disturbs the similarity conditions by changing material morphology (crystallinity), and mobility of aggressive agent. Moreover, the processes of AO extraction, consumption, and diffusion as well as various stages of fracture all have different temperature acceleration factors. It appears that different scaling laws operate on various stages of fracture process. The theoretical modeling formulated above allows one to sort out the above-mentioned factors and formulate an appropriate accelerated testing for different stages of fracture.

References

Allara, D.L., Hawkins, W.L., 1978. Advances in Chemistry Series. American Chemical Society, Washington DC.

Allen, N.S., 1983. Degradation and Stabilization of Polyolefins. Applied Science Publishers, London.

Anismov, M.P., 2003. Nucleation: theory and experiment. Russian Chemical Review 72 (7), 591–624.

Bishop, S., Issac, D.H., Hinksman, P., Morrissey, P., 2000. Environmental stress cracking of poly(vinyl chloride) in alkaline solutions. Polymer Degradation and Stability 70, 477–484.

Choi, B.-H., Chudnovsky, A., 2002. Stress corrosion crack growth in pipe grade steels in near neutral PH environment. International Journal of Fracture 116, L43–L48.

Choi, B.-H., Chudnovsky, A., Kin, Y., Teitsma, 2002. A., Observation and modeling of stress corrosion and fatigue corrosion cracking. In: Proceedings of Fatigue 2002. Stockholm, Sweden, pp. 3309–3313.

Chudnovsky, A., Kunin, B., 1987. A probabilistic model of brittle crack formation. Journal of Applied Physics 62 (10), 4124–4129.

Chudnovsky, A., Kunin, B., Gorelik, M., 1997. Modeling of brittle fracture based on the concept of crack trajectory ensemble. Engineering Fracture Mechanics 58 (5–6), 437–457.

Chudnovsky, A., 1973. In: Kachanov, L.M. (Ed.), Studies on Elasticity and Plasticity, vol. 9 (3–41). Leningrad University Press, Leningrad (in Russian).

Guven, O., 1990. NATO ASI Series, Series C: Mathematical and Physical Sciences, vol. 292. Kluwer Academic Publishers.

Ivanova, E., Chudnovsky, A., Wu, S., Bosnyak, C.P., 1995. In: Proceedings of ANTEC95. Boston, pp. 3893–3898.

Niu, X., Martynenko, E., Chudnovsky, A., Patel, S.H., Stivala, S.S., 2000, The effect of chemical degradation on physical properties and fracture behavior of poly (ethylene-co-carbon monoxide) and poly (1-butene). In: Proceedings of SPE/ANTEC 2000 III. Orlando, Florida, pp. 3228–3232.

Shames, I.H., Cozzarelli, F.A., 1992. Elastic and Inelastic Stress Analysis. Prentice Hall, Englewood Cliffs, NJ.

Volman, K.W., Cote-Verhaaf, A., Iling, R., 1996. Public inquiry concerning stress corrosion cracking on canadian oil and gas pipelines. National Energy Board Report of the Inquiry, MH-2-95.

Zhang, B., Gogotsi, Y., Chudnovsky, A., Teitsma, A., 1998. Thermodynamic analysis and experimental investigation of SCC in steel gas pipes. In: Proceeding of IGRC'98. pp. 607–617.

Zhang, B., Fan, J., Gogotsi, Y., Chudnovsky, A., Teitsma, A., 2000. Statistical and thermodynamic modeling of stress corrosion cracking in steel gas pipes. In: Proceeding of the Fourth International Symposium on Risk, Economy and Safety: Failure Minimization and Analysis. pp. 381–397.